



OPEN

High fat diet affects the hippocampal expression of miRNAs targeting brain plasticity-related genes

Matteo Spinelli^{1,2,7}, Francesco Spallotta^{3,4,7}, Chiara Cencioni⁵, Francesca Natale^{1,2}, Agnese Re^{5,6}, Alice Dellaria¹, Antonella Farsetti⁵, Salvatore Fusco^{1,2}✉ & Claudio Grassi^{1,2}

Metabolic disorders such as insulin resistance and type 2 diabetes are associated with brain dysfunction and cognitive deficits, although the underpinning molecular mechanisms remain elusive. Epigenetic factors, such as non-coding RNAs, have been reported to mediate the molecular effects of nutrient-related signals. Here, we investigated the changes of miRNA expression profile in the hippocampus of a well-established experimental model of metabolic disease induced by high fat diet (HFD). In comparison to the control group fed with standard diet, we observed 69 miRNAs exhibiting increased expression and 63 showing decreased expression in the HFD mice's hippocampus. Through bioinformatics analysis, we identified numerous potential targets of the dysregulated miRNAs, pinpointing a subset of genes regulating neuroplasticity that were targeted by multiple differentially modulated miRNAs. We also validated the expression of these synaptic and non-synaptic proteins, confirming the downregulation of Synaptotagmin 1 (SYT1), calcium/calmodulin dependent protein kinase I delta (CaMK1D), 2B subunit of N-methyl-D-aspartate glutamate receptor (GRIN2B), the DNA-binding protein Special AT-Rich Sequence-Binding Protein 2 (SATB2), and RNA-binding proteins Cytoplasmic polyadenylation element-binding protein 1 (CPEB1) and Neuro-oncological ventral antigen 1 (NOVA1) in the hippocampus of HFD mice. In summary, our study offers a snapshot of the HFD-related miRNA landscape potentially involved in the alterations of brain functions associated with metabolic disorders. By shedding light on the specific miRNA-mRNA interactions, our research contributes to a deeper understanding of the molecular mechanisms underlying the effects of HFD on the synaptic function.

Keywords MiRNAs, Cognitive decline, Brain plasticity, High fat diet, Hippocampus, Synaptic proteins

In recent decades, the prevalence of metabolic disorders such as insulin resistance and Type 2 Diabetes (T2D) has escalated globally, now ranking as the fourth leading cause of death in developed countries¹. The World Health Organization states that 422 million people live with diabetes, significantly stressing the national healthcare systems². Concurrently, rates of cognitive decline (CD) and dementia are increasing worldwide, with projections suggesting even higher incidences in developing countries. Emerging research suggests a positive correlation between metabolic dysregulation and CD in patients with T2D, increasing their vulnerability to dementia³. Multiple mechanisms have been proposed to explain the cognitive decline observed in metabolic disease, including nutrient overload leading to mitochondrial dysfunction, neuroinflammation caused by pro-inflammatory cytokine release, brain insulin resistance (BIR), and aberrant expression of synaptic plasticity-related genes⁴. However, the precise molecular underpinnings connecting T2D and CD remain elusive. Many studies suggested the potential role of small non-coding RNAs (miRNAs) in regulating glucose and lipid metabolism thus contributing to the multi-organ metabolic alterations observed in T2D and obesity⁵⁻⁸.

¹Department of Neuroscience, Università Cattolica del Sacro Cuore, 00168 Rome, Italy. ²Fondazione Policlinico Universitario A. Gemelli IRCCS, 00168 Rome, Italy. ³Department of Biology and Biotechnologies Charles Darwin, Sapienza University, 00185 Rome, Italy. ⁴Istituto Pasteur Italia-Fondazione Cenci Bolognetti, 00185 Rome, Italy. ⁵Institute for Systems Analysis and Computer Science "A. Ruberti", National Research Council (CNR-IASI), Rome, Italy. ⁶Dipartimento di Scienze Laboratoristiche ed Infettivologiche, UOC Chimica, Biochimica e Biologia Molecolare Clinica, Università Cattolica del Sacro Cuore, 00168 Rome, Italy. ⁷These authors contributed equally: Matteo Spinelli and Francesco Spallotta. ✉email: salvatore.fusco@unicatt.it

miRNAs are sequences of 18–25 nucleotides that are not translated into proteins and bind the 3'-untranslated region of their mRNA targets to post-transcriptionally regulate gene expression. Non-coding RNAs are highly expressed in the brain, and they are involved in the modulation of brain functions in both physiological and pathophysiological conditions⁹. miRNAs have been demonstrated to regulate molecular cascades underlying learning and memory¹⁰. Moreover, changes of miRNA expression have been reported in brain tissues of patients affected by dementia¹¹. However, the effect of metabolic disorders on the expression of both miRNAs and their targets inside the brain is largely unknown. Our study addressed this gap by analyzing the miRNA expression profile in the hippocampus of mice fed with high fat diet (HFD), a widely recognized experimental model of insulin resistance. We also performed a bioinformatic characterization of targets involved in the regulation of brain plasticity and potentially modulated by HFD-related hippocampal miRNome pattern. Finally, we validated several common targets of upregulated miRNAs in the hippocampus of HFD mice and we found the downregulation of synaptic and non-synaptic proteins (e.g., GRIN2B, SYT1, CaMKI delta, CPEB1, NOVA1, SATB2) regulating learning and memory. Our data provide an unbiased map of miRNAs potentially affecting brain functions in experimental models of metabolic diseases.

Results

HFD induces insulin resistance and cognitive deficits in mice

It has been widely established that metabolic disorders impair brain plasticity and cognitive function through multiple mechanisms that are not yet fully defined^{12,13}. To set up an experimental model of insulin resistance, we fed male mice with standard or high fat diet (SD or HFD, respectively) and evaluated the metabolic profile of the animals. At the end of the dietary regimen, HFD mice showed a greater weight (33.2 ± 0.9 g vs. 27.1 ± 0.6 g; $p = 1.6 \times 10^{-5}$, $n = 10$; Fig. 1A) and higher levels of both glycaemia and insulinemia (glycaemia: 8.02 ± 0.43 mmol/L vs. 5.64 ± 0.31 mmol/L, $p = 1.6 \times 10^{-4}$; insulinemia: 242.7 ± 15.9 pmol/L vs. 90.3 ± 5.9 pmol/L, $p = 2.1 \times 10^{-8}$; $n = 10$ for both analyses; Fig. 1B,C) compared to controls. Moreover, to quantify the HFD-related metabolic derangement, we calculated the homeostatic model assessment of insulin resistance (HOMA-IR) index in both cohorts of mice. HFD mice displayed a severe alteration of peripheral insulin sensitivity, indicating an impairment of glucose metabolism homeostasis (85.6 ± 6.4 vs. 22.6 ± 1.4 ; $p = 1.1 \times 10^{-8}$, $n = 10$; Fig. 1D). Afterwards, we studied the effects of HFD-dependent metabolic derangement on the hippocampus-related cognitive tasks by performing both novel object recognition and object place recognition tests (NOR and OPR, respectively). In parallel with metabolic signs of insulin resistance, HFD mice showed worse performance in both behavioural tests (NOR preference index: $56.4 \pm 1.1\%$ vs. $65.9 \pm 1.3\%$, $p = 1.5 \times 10^{-5}$; OPR preference index: $56.2 \pm 1.1\%$ vs. $66.6 \pm 1.4\%$,

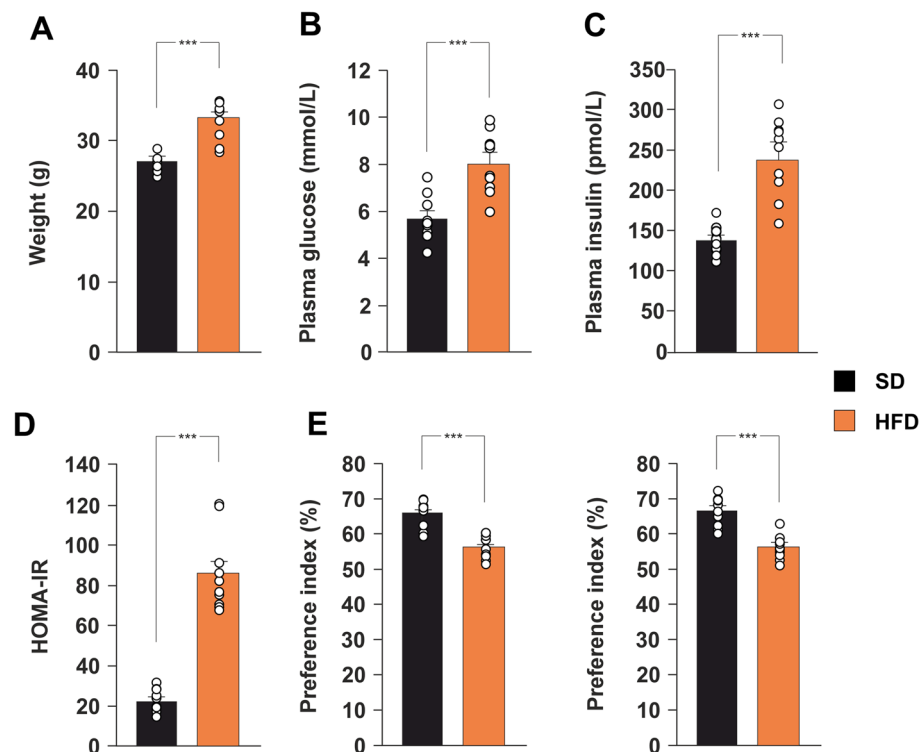


Figure 1. HFD causes metabolic alterations and impairment of hippocampus-dependent cognitive tasks. (A) Weight, (B) fasting glucose blood levels, (C) fasting insulin plasma levels, and (D) HOMA-IR score of SD and HFD mice ($n = 10$ per group; statistics by unpaired Student's *t*-test). (E) Preference index for novel object in the novel object recognition (left) and object place recognition (right) tests in SD and HFD mice ($n = 10$ per group; statistics by unpaired Student's *t*-test). Data are expressed as mean \pm SEM. *** $p < 0.001$.

$p = 8.3 \times 10^{-6}$; $n = 10$ for both tests; Fig. 1E), indicating that HFD-related metabolic changes significantly affected hippocampal function.

HFD alters the miRNA expression profile in the hippocampus

To investigate the potential contribution of miRNA dysregulation to insulin resistance-related cognitive impairment, we carried out an unbiased wide-spectrum analysis of hippocampal miRNome in both SD and HFD mice. Specifically, using TaqMan advanced miRNA array cards, we determined the profiles of 754 miRNAs in the hippocampus of 4 HFD- and 4 SD-fed mice. The comparison of miRNA profiles in the hippocampus according to dietary regimen classes identified a pool of miRNAs sensitive to dysmetabolism, whose expression is altered in the hippocampus of HFD-fed mice (Table 1).

CARD A (HFD Vs SD)		CARD B (HFD Vs SD)	
miRBase ID (v22) or NCBI Name (for Controls)	$-\log_2(\text{Fold change})$	miRBase ID (v22) or NCBI Name (for Controls)	$-\log_2(\text{Fold change})$
mmu-miR-511-5p	4.64	rno-miR-25-5p	5.99
mmu-miR-465a-5p	3.75	mmu-miR-34b	3.76
mmu-miR-1a-3p	3.41	mmu-miR-1897-5p	3.68
mmu-miR-351-5p	3.32	mmu-miR-763	3.53
rno-miR-196c-5p	2.55	mmu-miR-33-3p	3.07
mmu-miR-467d-5p	2.36	mmu-let-7f.-1-3p	2.61
rno-miR-224	2.14	mmu-miR-127-5p	2.54
mmu-miR-211-5p	2.09	mmu-miR-880-3p	2.38
mmu-miR-465b-5p	1.84	mmu-miR-721	2.21
mmu-miR-452-5p	1.80	mmu-miR-1897-3p	2.17
mmu-let-7f.-5p	1.80	mmu-miR-1928	2.14
rno-miR-743b-3p	1.64	mmu-miR-715	2.03
mmu-miR-742-3p	1.60	mmu-miR-1191	2.02
mmu-miR-20b-5p	1.50	mmu-miR-30c-2-3p	1.84
mmu-miR-542-3p	-1.56	rno-miR-99a-3p	1.80
mmu-miR-182-5p	-1.58	rno-miR-489	1.79
mmu-miR-25-3p	-1.64	mmu-miR-712-5p	1.78
mmu-miR-367-3p	-1.76	mmu-miR-1906	1.62
mmu-miR-490-3p	-1.92	mmu-miR-694	1.61
mmu-miR-873a-5p	-1.92	mmu-miR-326-3p	1.56
mmu-miR-542-5p	-1.92	rno-miR-28-3p	1.54
rno-miR-871	-1.94	mmu-let-7i-3p	1.53
mmu-miR-467c-5p	-2.32	mmu-miR-1947-5p	1.52
mmu-miR-802-5p	-2.37	mmu-miR-27b-5p	-1.51
mmu-miR-208b-3p	-2.39	mmu-miR-673-5p	-1.51
mmu-miR-743b-5p	-3.51	mmu-miR-141-5p	-1.54
mmu-miR-216a-5p	-3.88	mmu-miR-804	-1.54
mmu-miR-200c-3p	-4.16	mmu-miR-706	-1.71
mmu-miR-105	-4.18	mmu-miR-1930-5p	-1.76
mmu-miR-377-3p	-5.16	mmu-miR-200b	-1.77
mmu-miR-466 h-5p	-8.38	mmu-miR-1941-5p	-2.09
		mmu-miR-338-5p	-2.11
		mmu-let-7b-3p	-2.22
		mmu-miR-669c-5p	-2.28
		mmu-miR-374b-3p	-2.33
		mmu-miR-712-3p	-2.38
		mmu-miR-483-3p	-2.44
		mmu-miR-376a-5p	-3.17
		mmu-miR-1193-3p	-3.97
		mmu-miR-2136	-5.44
		mmu-miR-325-5p	-7.38

Table 1. List of the most upregulated miRNAs in the hippocampus of HFD mice ($-1.5 < -\log_{10}(\text{FC}) < 1.5$) ($n = 3$ per group).

More specifically, we found 37 upregulated miRNAs (fold change > 1.5) and 35 downregulated miRNAs (fold change < 1.5) in the hippocampus of HFD mice in comparison to the SD group (Supplementary Table 1). Profiling data showed an equal distribution between up- and down-modulated differentially expressed miRNAs in the hippocampus of both SD and HFD mice. Taken together, the miRNome analysis revealed a significant HFD-dependent derangement of miRNA expression in the hippocampus of mice.

HFD-related miRNAs target synaptic and non-synaptic proteins regulating brain plasticity

Once identified the hippocampal miRNAs sensitive to HFD, miRNA-target interactions were analyzed using the online available tool MicroRNA Enrichment TURNed NETWORK (MIENTURNET; <http://userver.bio.uniroma1.it/apps/mienturnet/>)³⁴, focusing on the list of predicted target genes, highlighted by TargetScan, of the identified up-regulated miRNAs. The gathered list of predicted target genes of the hippocampal miRNome associated with HFD-dependent metabolic derangement included 256 genes. These were further investigated by the online available tool Database for Annotation, Visualization and Integrated Discovery (DAVID; <https://david.ncifcrf.gov/>) to assess their role in the alteration of memory and response to insulin observed in mice fed with HFD. The performed gene ontology analysis restricted the list of genes of interest to 88 involved in biological processes related to neurobiology (Fig. 2A). The network visualization by MIENTURNET allowed us to evaluate the number of interactions among the identified up-regulated miRNAs and the predicted targeted genes, highlighting a set of 9 miRNAs highly recurrent in the network with 266 targets, including miR1a (117 interactions), miR34b (100 interactions), miR211 (142 interactions), miR224 (70 interactions), miR351 (104 interactions), miR452 (77 interactions), miR489 (69 interactions), miR721 (136 interactions) and miR1928 (104 interactions) (Fig. 2B). A particular focus on “neuro”-associated targets identified a list of synaptic plasticity-related genes targeted by minimum 3 upregulated miRNAs, including Camk1d, Cpeb2, Creb1, Foxp2, Grin2a, Grin2b, Nova1, Sat2, Snap25, and Syt1, which were further analyzed in dedicated wet lab experiments.

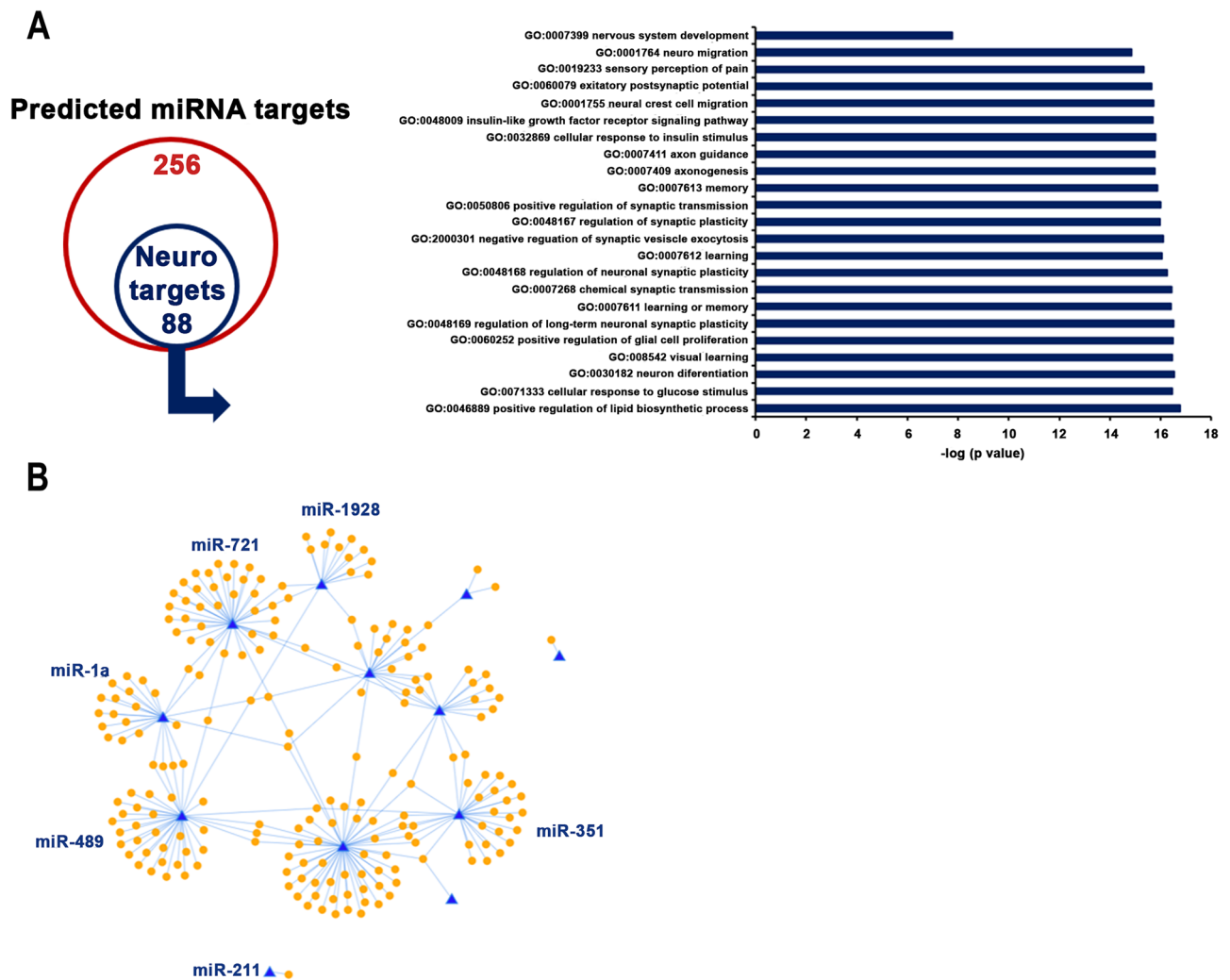


Figure 2. HFD-related miRNAs target synaptic and non-synaptic proteins regulating brain plasticity. (A) Gene ontology analysis of predicted miRNA targets selected according to their role in neurobiology. (B) Network interaction between upregulated miRNAs and identified neuro targets.

The expression of upregulated miRNA targets is inhibited in the hippocampus of HFD mice

To validate the in-silico results and to evaluate the impact of HFD-related miRNome alterations on brain function, we analyzed the expression of several synaptic and non-synaptic targets of miRNAs that were upregulated in the hippocampus of HFD mice. First, we investigated the expression of synaptic proteins, which the bioinformatic analysis selected as targets of at least three overexpressed miRNAs. We found a significant decrease of both pre-synaptic and post-synaptic proteins, i.e., synaptotagmin 1 (SYT1), calcium/calmodulin dependent protein kinase I delta (CaMK1-D) and 2B subunit of N-methyl-D-aspartate glutamate receptor (GRIN2B) in the hippocampus of overfed mice (SYT1: -59.6%, $p=0.007$; CaMK1D: -48.9%, $p=0.006$; GRIN2B: -60.2%, $p=0.04$; $n=6$; Fig. 3A). No significant changes were detected for GRIN2A, Synaptosome-associated protein of 25 kDa (SNAP25), and SEPTIN3. Moreover, we analyzed the expression of other non-synaptic proteins targeted by dysregulated miRNAs and potentially involved in regulating brain plasticity and cognitive function. Immunoblot analysis revealed a significant downregulation of the RNA-binding proteins Cytoplasmic polyadenylation element-binding protein 1 (CPEB1) and Neuro-oncological ventral antigen 1 (NOVA1), and the DNA-binding protein Special AT-Rich Sequence-Binding Protein 2 (SATB2) in the hippocampus of HFD mice (CPEB1: -57.7%, $p=0.03$; NOVA1: -67%, $p=0.01$; SATB2: -59%, $p=0.01$; $n=6$; Fig. 3B). We also detected a non-statistically significant decrease of transcription factors Forkhead box protein P2 (FOXP2) and cAMP response element-binding protein (CREB) (FOXP2: -32%, $p=0.2$; CREB: -35.9%, $p=0.08$; $n=6$; Fig. 3B). Collectively, our findings identified a group of molecular targets that were downmodulated by HFD-dependent upregulated miRNAs and potentially involved in the insulin resistance-related brain alterations.

Discussion

Metabolic disorders, such as obesity, insulin resistance and T2D, have been shown to induce multi-organ damage via multiple mechanisms including oxidative stress, inflammatory responses, insulin signalling alteration and vascular dysfunction^{13,14}. The role of epigenetic modifications in the onset and progression of these metabolic disorders is a growing area of interest^{15,16}. Changes in DNA methylation, chromatin histone modifications, and non-coding RNAs have been implicated in the pathogenesis of metabolic disorder-related organ loss of function such as diabetic nephropathy¹⁷. Furthermore, miRNAs have been reported to exacerbate mitochondrial dysfunction in diabetic neuropathy¹⁸, while non-coding RNAs targeting inflammation and oxidative stress pathways have been implicated in T2D complications such as retinopathy, nephropathy, and vascular issues^{19,20}. Brain is emerging as a highly vulnerable organ to metabolic stress^{4,21}. Here, we demonstrated that HFD induced insulin resistance, cognitive deficits and alteration of miRNA expression profile in the mouse hippocampus, which is a key brain region for cognitive function. We focused our attention on male mice because previous reports documented that male brain is more susceptible to metabolic changes induced by HFD²² and we already demonstrated how short-term HFD affected synaptic plasticity and memory in male mice²³. Moreover, changes of both hormone profile and microbiota have been demonstrated to influence multiorgan responses to HFD in female mice^{24–26}. Bioinformatic analysis of HFD-related miRNome revealed dysregulation of miRNAs targeting pathways regulating synaptic function and involved in neurodegeneration associated with alteration of glucose homeostasis pathways. Gene ontology analysis also identified potential gene targets of upregulated miRNAs, which were involved in the modulation of both synaptic plasticity and insulin receptor (IR) downstream intracellular signalling. This finding allowed us to narrow down the target genes with relevance to their roles at crossroad between metabolic stress and alteration of brain plasticity. We previously showed that short-term HFD induced brain insulin resistance and affected both basal and insulin-dependent activation of IR downstream effectors²³. However, we cannot rule out that miRNA profile changes in hippocampi of overfed mice may be due to HFD-related signals other than the insulin molecular cascade. For instance, HFD has been reported to increase pro-inflammatory cytokines in the hippocampus²⁷. It has been also demonstrated that obesogenic diets alter leptin and IGF-1 signalling inside the brain leading to changes of miRNA expression^{28–30}. Then, we selected ten synaptic and non-synaptic proteins potentially modulated by the most recurrently upregulated miRNAs in our network analysis of the HFD-fed mouse hippocampus. Western blotting analysis confirmed the downregulation of several synaptic proteins (i.e., SYT1, CaMK1D, GRIN2B) and non-synaptic targets regulating RNA metabolism (i.e., CPEB1, NOVA1, SATB2). Notably, altered expressions of miRNAs implicated in the regulation of proteins involved in AD (e.g., APP, BACE1, and tau) have been found in the hippocampus of AD patients, suggesting a role for miRNAs in the onset and progression of cognitive impairment^{31,32}. Accordingly, miRNA dysregulation in the HFD brain might contribute to affect cognitive function by inhibiting the expression of neuronal enzymes regulating synaptic activity³³.

Furthermore, alterations in non-coding RNA expression could impinge on different pathways regulating brain plasticity including mitochondrial function, autophagy, protein homeostasis and neuroinflammation^{34–36}. Non-coding RNAs might also impair brain insulin sensitivity by affecting insulin receptor downstream effectors such as PTEN/PI3K/Akt signalling, mTOR, AMPK, or NF- κ B pathways³⁷.

A greater knowledge of the regulatory role of miRNAs in cognitive functions could be essential to understand how metabolic diseases impact on cognitive impairments. Furthermore, understanding the role of miRNAs in the brain will help to develop potential new diagnostic strategies (i.e., gene therapy) applicable in metabolic disorders and aging-associated cognitive alterations. A growing body of research supports not only a role for epigenetics in disease development, but also epigenetic changes as a response to disease. This speculation paved the way to the study of non-coding RNAs as biomarkers of human diseases³⁸. The recent development of molecular strategies to selectively isolate brain-derived extracellular vesicles containing miRNAs from biological fluids provides a good starting point for follow-up studies exploring the possibility to identify predictive biomarkers, such as non-coding RNAs, for HFD-related brain dysfunction^{39,40}. Finally, miRNAs released from tissues can play an active role in the inter-organ crosstalk in physiology and disease⁴¹. Our findings do not provide evidence of a causal relationship

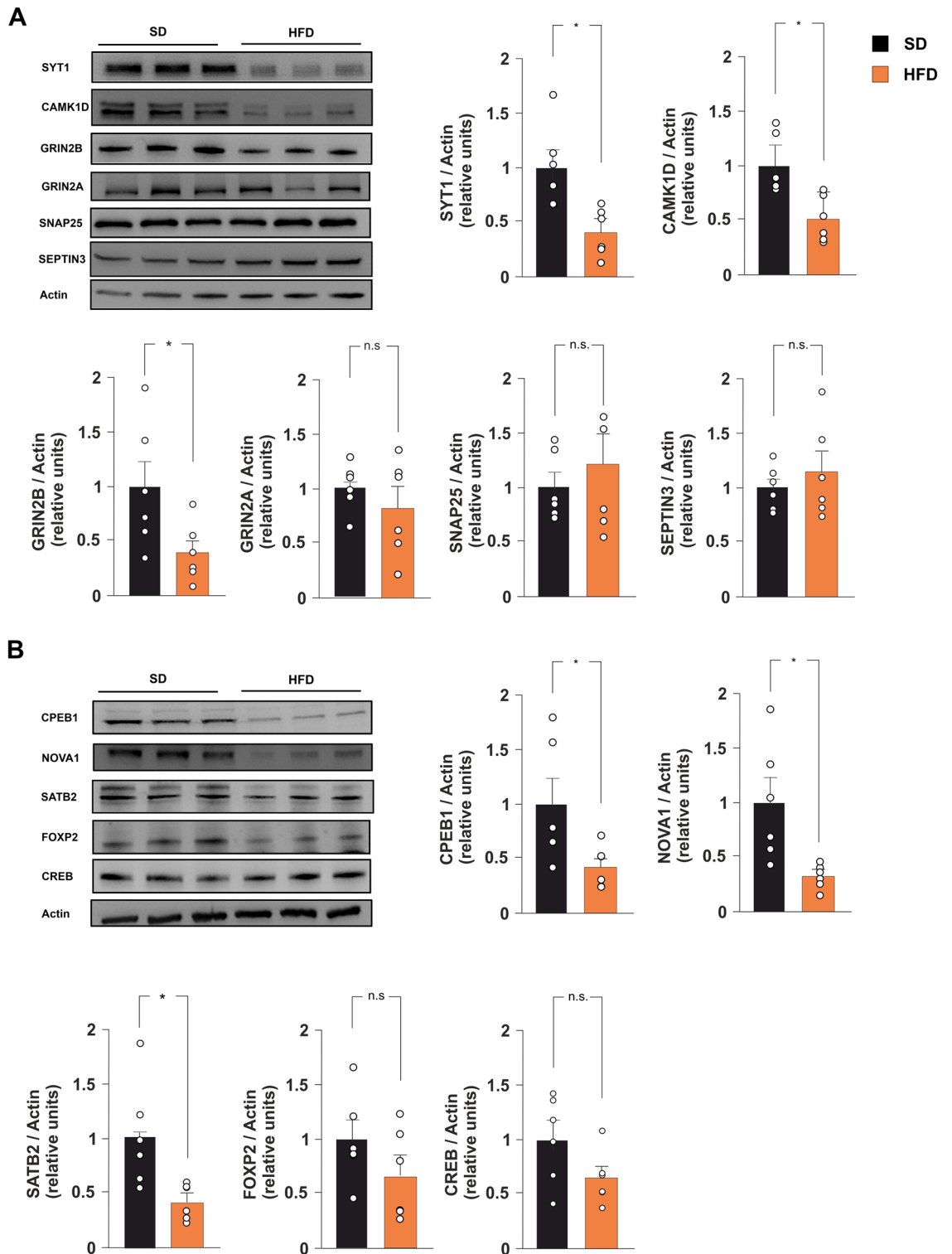


Figure 3. HFD inhibits the expression of synaptic and non-synaptic proteins targeted by upregulated miRNAs. (A) Immunoblots and bar graphs showing the expression of SYT1, CAMK1D, GRIN2B, GRIN2A, SNAP25, and SEPTIN3 in the hippocampi of SD and HFD mice (n=6 per group; statistics by unpaired Student’s t-test). (B) Immunoblots and bar graphs showing the expression of CPEB1, NOVA1, SATB2, FOXP2, and CREB in the hippocampi of SD and HFD mice. (n=6 per group; statistics by unpaired Student’s t-test). Original blots/gels are presented in Supplementary Fig. 1. Data are expressed as mean ± SEM. *p < 0.05; n.s. not significant.

among the HFD-induced upregulation of miRNAs, the hippocampal downregulation of synaptic proteins and memory deficits. However, the present study provides an unprecedented molecular map of miRNA alterations induced in the hippocampus of an experimental model of metabolic disease. Future studies will be necessary to evaluate the impact of dysregulated miRNAs in neuronal and glial molecular pathways and to investigate their critical role in the HFD-related synaptic and memory deficits.

Methods

Ethics approval

This study was performed in line with the principles of the Declaration of Helsinki. All animal procedures underwent review and approval by the Ethics Committee of Università Cattolica del Sacro Cuore and Italian Ministry of Health on November 14, 2020 (date: 14 November 2020; authorization number: 1113/2020-PR). These procedures adhered fully to the guidelines established by the Italian Ministry of Health (Legislative Decree No. 116/1992) and the European Union (Directive 2010/63/EU for animal experiments) regarding animal research. The procedures comply with the ARRIVE guidelines and were in accordance with the U.K. Animals (Scientific Procedures) Act, 1986 and associated guidelines. The approved guidelines were strictly followed during the execution of the methods.

Animals

21–24 day-old male C57BL/6 mice, procured from the Animal Facility of Università Cattolica del Sacro Cuore, were utilized in this study. The mice were randomly assigned to one of two feeding regimens: (i) a standard diet (SD) serving as the control group, and (ii) a high-fat diet (HFD) group. Each experimental test employed distinct groups of mice. Throughout the study, the mice were housed in groups, with 3 to 5 animals per cage, and they were subject to daily monitoring. The mice were housed under standardized conditions, with a 12 h light–dark cycle and a room temperature range of 19–22 °C. They were fed with their respective diets and water ad libitum, while their weight was weekly monitored.

Treatments

Mice from the same litter were randomly divided into various experimental groups and fed with different dietary regimens for 8 weeks. One group received a standard diet (SD) consisting of 18.5% proteins, 46% carbohydrates (including 42% starch and 4% sucrose), and 3% fats, with a fat caloric content of 6.55% (catalog number 4RF21). Another group received a high-fat diet (HFD) containing 23% proteins, 42% carbohydrates (including 28% starch, 9% sucrose, and 5% maltodextrin), and 34% fats, with a fat caloric content of 60% (catalog number PF4051/D). Both diets were provided by Mucedola, located in Guidonia Montecelio, RM, Italy.

For molecular analyses, some mice were chosen and immediately sacrificed after the diet period. These sacrificed mice were used to obtain data and information through molecular analysis techniques.

Metabolic analyses

Metabolic analyses were performed at the end of dietary regimen and in fasting conditions. Blood glucose level was measured through a glucometer by placing a small drop of blood tail on test strip. Plasma insulin levels were determined by using a commercially available Elisa kit (Immunological Sciences). Blood samples were collected from the retro-orbital plexus with sterile glass Pasteur pipettes. Plasma was separated by centrifugation and stored at –80 °C until further use. The assay was performed according to the manufacturer's instructions. The HOMA-IR test is used to assess animal glucose metabolism. The animals are first subjected to a fasting period of approximately 16 h. The HOMA-IR is calculated to evaluate insulin resistance. This calculation involves multiplying the fasting plasma insulin levels (measured in picomoles per liter) by the fasting plasma glucose levels (measured in millimoles per liter) and dividing the product by 22.5.

Behavioural tests

The behavioural tests conducted were designed to evaluate various aspects of memory and cognition in mice. The tests were performed between 9 a.m. and 4 p.m., ensuring consistent conditions throughout the experiments. To ensure unbiased data, the collected data were analyzed blindly using an automated video tracking system called Any-Maze™. Recognition memory was assessed using a novel object recognition test as previously reported⁴². The test consisted of three consecutive days of experimentation. On the first day, the animals were familiarized with the test arena, which measured 45 × 45 cm for 10 min. This procedure allowed the mice to acclimate to the environment without any objects. On the second day, referred to as the training session, the mice were introduced to the arena again. This time, two identical objects were symmetrically placed within the arena. The mice were given 10 min to explore the objects freely. It is important to note that mice meeting specific criteria were included in the subsequent test session. Any mouse that exhibited a total exploration time of fewer than 20 s or spent more than 10% of the total exploration time focused on only one of the two identical objects during the training session was excluded from further analysis. On the third day (test session), one of the old objects was replaced with a novel object. The mice were given another 10 min exploration period. To eliminate any potential bias based on the location of the objects, the position of the novel object was alternated on both sides of the box between different trials. This ensured that the mice were not simply exhibiting a place preference but were truly recognizing the novelty of the object. The preference index, calculated as the ratio of time spent exploring the novel object to the total exploration time of both objects, served as a quantitative measure of recognition memory. After each test, the objects and the test arena were thoroughly cleaned using a 70% ethanol solution to remove any olfactory cues. The distances travelled in the behavioural arena were analyzed to rule out changes in locomotor activity between the experimental groups.

Spatial memory was assessed using an object place recognition (OPR) test. Prior to the actual testing phase, the animals underwent a 10 min habituation period in the testing arena. Spatial cues were strategically placed on the arena's walls, providing the mice with spatial points of reference. After the habituation phase, the training phase commenced approximately 24 h later. Two identical objects were placed in opposite corners of the arena, and the mice were allowed to explore for 10 min. Following the exploration period, the animals were removed from the testing arena and returned to their home cages. The following day, a spatial memory test was conducted. One of the objects from the training phase was moved to the opposite corner of the arena. The mice were reintroduced to the testing area and given 10 min to explore the objects. Like the novel object recognition test, the time spent exploring both objects was recorded, and a preference index for the displaced object was calculated. Between each mouse's trial, the objects and the arena were meticulously cleaned using a 70% ethanol solution, and fresh bedding was added to eliminate potential residual cues. By employing these comprehensive behavioral tests, the researchers aimed to gain insights into the mice's recognition memory and spatial memory capabilities. The rigorous protocols and cleaning procedures ensured the reliability and accuracy of the data collected during the study.

RNA extraction and miRNA profiling by TaqMan array cards

According to the Qiagen protocol, miRNAs were extracted from SD and HFD mice hippocampal samples using Qiagen miRNeasy mini kit (Qiagen, GmbH, Hilden, Germany). RNA was eluted in 30 μ l of elution buffer with two repeated steps in the same collection tube. RNAs were quantified by spectrophotometry (Nanodrop 1000, ThermoFisher Scientific, Waltham, MA, USA). According to the manufacturer's instructions, 30 ng of RNAs were reverse transcribed into cDNA using Megaplex™ RT Primers (ThermoFisher Scientific, Waltham, MA, USA) and cDNA was pre-amplified to increase its quantity in two separate reactions for Megaplex™ PreAmp Primers Pool A and Pool B (ThermoFisher Scientific, Waltham, MA, USA). Negative control was used for each preamplification. For each sample, a qPCR reaction was prepared by mixing: 9 μ l of single preamplification product, 441 μ l nuclease-free water, 450 μ l TaqMan Universal Master Mix, and no AmpErase UNG. Next, the qPCR reaction mixes with samples were loaded to each fill reservoir of the TaqMan Array Cards A (Catalog number 4398967) and B (Catalog number 4444899). Ready Cards were run into the 7900HT Fast Real-time PCR System with Array block and processed with Threshold (Ct) algorithm. The miRNAome analysis was performed according to the software provided by Thermo Fisher (Thermo Fischer cloud dashboard) related to TaqMan Array Cards A (Catalog number 4398967) and B (Catalog number 4444899). Normalization was performed on a pool of 5 non-coding RNAs present into the two cards, whose expression resulted stable in all experimental conditions: U6 snoRNA, snoRNA135, Y1, snoRNA202 and U87 snoRNA.

Network construction and analysis

To evaluate the biological meaning of differentially expressed miRNAs, we retrieved their experimentally validated targets by MIENTURNET (<http://userver.bio.uniroma1.it/apps/mienturnet/>), an interactive web tool for microRNA-target enrichment and network-based analysis developed to predict targets of microRNAs and their miRNA-target interactions⁴³. To identify the associated target gene signaling regulated by differentially expressed miRNAs related to neuronal plasticity, we performed a gene ontology analysis by DAVID Go (<https://david.ncifcrf.gov/>) on the predicted differentially expressed miRNA targets and selected only the list of miRNA-target genes accounted in the GO id associated with neuronal plasticity. Statistical over-representation was calculated using Fisher's exact test; Benjamini & Hochberg FDR Correction; $p < 0.005$.

Western blotting

Tissues were subjected to lysis using ice-cold lysis buffer, composed of 150 mM NaCl, 50 mM Tris-HCl (pH 7.4), and 2 mM EDTA. The lysis buffer also contained 1% Triton X-100, 0.1% SDS, 1 \times protease inhibitor cocktail, 1 mM sodium orthovanadate, and 1 mM sodium fluoride, following the previously described protocol⁴⁴. The lysates were incubated on ice at 4 °C with intermittent vortexing for 10 min, followed by sonication on ice for 5 min. Subsequently, the homogenates were centrifuged at 13,000 \times g for 15 min at 4 °C. The protein content in the resulting supernatant was quantified using the Bradford assay (DC Protein Assay; Bio-Rad). Approximately 40–60 μ g of proteins from the total lysates were diluted in Laemmli buffer and boiled at 100 °C for 5 min. The protein samples were then separated using SDS-PAGE polyacrylamide gel. Each nitrocellulose membrane was divided into two parts and probed with antibodies targeting proteins of distinct molecular weights. In cases where necessary, the membranes were stripped before re-probing, with a maximum of one stripping performed. The primary antibodies, diluted in TBS-Tween20 and 3% non-fat dried milk at a concentration of 1 μ g/mL, were incubated overnight at 4 °C on a plate shaker. The proteins of interest were visualized using horseradish peroxidase-conjugated secondary antibodies (1:5000 in TBS-Tween20, Cell Signaling Technology Inc., Danvers, MA, USA). Protein expression levels were analyzed using UVItec Cambridge Alliance Software. The presented images were cropped for clarity, with no further alterations. The complete, unedited blots can be found in the supplementary files (Supplementary Fig. 1). Detailed information regarding the antibodies can be found in Supplementary Table 2.

Statistics

Sample sizes were chosen with adequate power (0.8) according to preliminary results of previous studies, including our own, which used similar methods or paradigms. Sample estimation and statistical analyses were performed using SigmaPlot 14 software. Data were first tested for equal variance and normality (Shapiro–Wilk test) and the appropriate statistical tests were chosen. The statistical tests used for each experiment are reported in the corresponding figure legends. N numbers are indicated in the main text and in the corresponding figure

legends. Degrees of freedom are $n-1$ for each condition. All statistical tests were two-tailed, and the level of significance was set at 0.05. Results are shown as mean \pm SEM.

Data availability

All data generated or analysed during this study are included in this published article and its supplementary information files.

Received: 22 February 2024; Accepted: 6 August 2024

Published online: 23 August 2024

References

- Guariguata, L. *et al.* Global estimates of diabetes prevalence for 2013 and projections for 2035. *Diabetes Res. Clin. Pract.* **103**, 137–49. <https://doi.org/10.1016/j.diabres.2013.11.002> (2014).
- NCD Risk Factor Collaboration (NCD-RisC). Worldwide trends in diabetes since 1980: A pooled analysis of 751 population-based studies with 4.4 million participants. *Lancet*. **387**(10027), 15131–530. [https://doi.org/10.1016/S0140-6736\(16\)00618-8](https://doi.org/10.1016/S0140-6736(16)00618-8) (2016).
- Cukierman-Yaffe, T. The relationship between dysglycemia and cognitive dysfunction. *Curr. Opin. Invest. Drugs*. **10**, 70–74 (2009).
- Spinelli, M., Fusco, S. & Grassi, C. Brain insulin resistance impairs hippocampal plasticity. *Vitam. Horm.* **114**, 281–306. <https://doi.org/10.1016/bs.vh.2020.04.005> (2020).
- Rottiers, V. & Näär, A. M. MicroRNAs in metabolism and metabolic disorders. *Nat. Rev. Mol. Cell Biol.* **13**, 239–250. <https://doi.org/10.1038/nrm3328> (2012).
- Agbu, P. & Carthew, R. W. MicroRNA-mediated regulation of glucose and lipid metabolism. *Nat. Rev. Mol. Cell Biol.* **22**, 425–438. <https://doi.org/10.1038/s41580-021-00354-w> (2021).
- Vienberg, S., Geiger, J., Madsen, S. & Dalgaard, L. T. MicroRNAs in metabolism. *Acta. Physiol. (Oxf)* **219**(2), 346–361. <https://doi.org/10.1111/apha.12681> (2017).
- Kato, M. & Natarajan, R. Epigenetics and epigenomics in diabetic kidney disease and metabolic memory. *Nat. Rev. Nephrol.* **15**, 327–345. <https://doi.org/10.1038/s41581-019-0135-6> (2019).
- Olsen, L., Klausen, M., Helboe, L., Nielsen, F. C. & Werge, T. MicroRNAs show mutually exclusive expression patterns in the brain of adult male rats. *PLoS ONE* **4**, e7225. <https://doi.org/10.1371/journal.pone.0007225> (2009).
- Wang, W., Kwon, E. J. & Tsai, L. H. MicroRNAs in learning, memory, and neurological diseases. *Learn Mem.* **19**(9), 359–368. <https://doi.org/10.1101/lm.026492.112> (2012).
- Takousis, P. *et al.* Differential expression of microRNAs in Alzheimer's disease brain, blood, and cerebrospinal fluid. *Alzheimer's Dement.* **15**, 1468–1477. <https://doi.org/10.1016/j.jalz.2019.06.4952> (2019).
- Spinelli, M., Fusco, S. & Grassi, C. Brain insulin resistance and hippocampal plasticity: Mechanisms and biomarkers of cognitive decline. *Front. Neurosci.* **13**, 788. <https://doi.org/10.3389/fnins.2019.00788> (2019).
- Mendrick, D. L. *et al.* Metabolic syndrome and associated diseases: From the bench to the clinic. *Toxicol. Sci.* **162**, 36–42. <https://doi.org/10.1093/toxsci/kfx233> (2018).
- Daryabor, G., Atashzar, M. R., Kabelitz, D., Meri, S. & Kalantar, K. The effects of type 2 diabetes mellitus on organ metabolism and the immune system. *Front. Immunol.* **11**, 1582. <https://doi.org/10.3389/fimmu.2020.01582> (2020).
- Ling, C. & Rönn, T. Epigenetics in human obesity and type 2 diabetes. *Cell Metab.* **29**, 1028–1044. <https://doi.org/10.1016/j.cmet.2019.03.009> (2019).
- Landrier, J. F., Derghal, A. & Mounien, L. MicroRNAs in obesity and related metabolic disorders. *Cells* **8**, 859. <https://doi.org/10.3390/cells8080859> (2019).
- Kato, M. & Natarajan, R. Diabetic nephropathy—emerging epigenetic mechanisms. *Nat. Rev. Nephrol.* **10**, 517–530. <https://doi.org/10.1038/nrneph.2014.116> (2014).
- Spallone, V., Ciccacci, C., Latini, A. & Borgiani, P. What Is in the field for genetics and epigenetics of diabetic neuropathy: The role of microRNAs. *J. Diabetes Res.* **2021**, 5593608. <https://doi.org/10.1155/2021/5593608> (2021).
- Kaur, P., Kotru, S., Singh, S. & Munshi, A. miRNA signatures in diabetic retinopathy and nephropathy: Delineating underlying mechanisms. *J. Phys. Biochem.* **78**, 19–37. <https://doi.org/10.1007/s13105-021-00867-0> (2022).
- Tanwar, V. S., Reddy, M. A. & Natarajan, R. Emerging role of long non-coding RNAs in diabetic vascular complications. *Front. Endocrinol.* **12**, 665811. <https://doi.org/10.3389/fendo.2021.665811> (2021).
- Arshad, N., Lin, T. S. & Yahaya, M. F. metabolic syndrome and its effect on the brain: Possible mechanism. *CNS Neurol. Disord. Drug Targe.* **17**, 595–603. <https://doi.org/10.2174/1871527317666180724143258> (2018).
- Murtaj, V. *et al.* Brain sex-dependent alterations after prolonged high fat diet exposure in mice. *Commun. Biol.* <https://doi.org/10.1038/s42003-022-04214-x> (2022).
- Saxena, A. *et al.* Sex differences in the fecal microbiome and hippocampal glial morphology following diet and antibiotic treatment. *PLoS One*. **17**(4), e0265850. <https://doi.org/10.1371/journal.pone.0265850> (2022).
- Hetty, S. *et al.* Sex-specific role of high-fat diet and stress on behavior, energy metabolism, and the ventromedial hypothalamus. *Biol. Sex Differ.* **15**(1), 55. <https://doi.org/10.1186/s13293-024-00628-w> (2024).
- Muralidharan, A. *et al.* Sex-specific effects of THR β signaling on metabolic responses to high fat diet in mice. *Endocrinology* **165**(8), bqae075. <https://doi.org/10.1210/endo/bqae075> (2024).
- Spinelli, M. *et al.* Brain insulin resistance impairs hippocampal synaptic plasticity and memory by increasing GluA1 palmitoylation through FoxO3a. *Nat. Commun.* **8**(1), 2009. <https://doi.org/10.1038/s41467-017-02221-9> (2017).
- Hersey, M. *et al.* High-fat diet induces neuroinflammation and reduces the serotonergic response to escitalopram in the hippocampus of obese rats. *Brain Behav. Immun.* **96**, 63–72. <https://doi.org/10.1016/j.bbi.2021.05.010> (2021).
- Sangiao-Alvarellos, S., Pena-Bello, L., Manfredi-Lozano, M., Tena-Sempere, M. & Cordido, F. Perturbation of hypothalamic microRNA expression patterns in male rats after metabolic distress: Impact of obesity and conditions of negative energy balance. *Endocrinology* **155**(5), 1838–1850. <https://doi.org/10.1210/en.2013-1770> (2014).
- Mainardi, M. *et al.* Loss of leptin-induced modulation of hippocampal synaptic transmission and signal transduction in high-fat diet-fed mice. *Front. Cell Neurosci.* **28**(11), 225. <https://doi.org/10.3389/fncel.2017.00225> (2017).
- Wang, F. *et al.* Inhibition of miR-129 Improves neuronal pyroptosis and cognitive impairment through IGF-1/GSK3 β signaling pathway: An in vitro and in vivo study. *J. Mol. Neurosci.* **71**(11), 2299–2309. <https://doi.org/10.1007/s12031-021-01794-x> (2021).
- Yang, G. *et al.* MicroRNA-29c targets β -site amyloid precursor protein-cleaving enzyme 1 and has a neuroprotective role in vitro and in vivo. *Mol. Med. Rep.* **12**, 3081–3088. <https://doi.org/10.3892/mmr.2015.3728> (2015).
- Lee, K. *et al.* Kim H (2016) Replenishment of microRNA-188-5p restores the synaptic and cognitive deficits in 5XFAD mouse model of Alzheimer's Disease. *Sci. Rep.* **6**, 34433. <https://doi.org/10.1038/srep34433> (2016).
- Song, M. (2020) miRNAs-dependent regulation of synapse formation and function. *Genes Genom.* **42**(8), 837–845. <https://doi.org/10.1007/s13258-020-00940-w> (2020).

34. Gowda, P., Reddy, P. H. & Kumar, S. Deregulated mitochondrial microRNAs in Alzheimer's disease: Focus on synapse and mitochondria. *Ageing Res. Rev.* **73**, 101529. <https://doi.org/10.1016/j.arr.2021.101529> (2022).
35. Van Dyken, P. & Lacoste, B. Impact of metabolic syndrome on neuroinflammation and the blood-brain barrier. *Front. Neurosci.* **12**, 930. <https://doi.org/10.3389/fnins.2018.00930> (2018).
36. Lapiere, L. R., Kumsta, C., Sandri, M., Ballabio, A. & Hansen, M. Transcriptional and epigenetic regulation of autophagy in aging. *Autophagy* **11**, 867–880. <https://doi.org/10.1080/15548627.2015.1034410> (2015).
37. Moayedi, K. *et al.* A novel approach to type 3 diabetes mechanism: The interplay between noncoding RNAs and insulin signaling pathway in Alzheimer's disease. *J. Cell Physiol.* **237**, 2838–2861. <https://doi.org/10.1002/jcp.30779> (2022).
38. Natale, F., Fusco, S. & Grassi, C. Dual role of brain-derived extracellular vesicles in dementia-related neurodegenerative disorders: Cargo of disease spreading signals and diagnostic-therapeutic molecules. *Transl. Neurodegener.* **11**(1), 50. <https://doi.org/10.1186/s40035-022-00326-w> (2022).
39. Fiandaca, M. S. *et al.* Identification of preclinical Alzheimer's disease by a profile of pathogenic proteins in neurally derived blood exosomes: A case-control study. *Alzheimers Dement.* **11**, 600–607. <https://doi.org/10.1016/j.jalz.2014.06.008> (2015).
40. Goetzl, E. J. *et al.* Cargo proteins of plasma astrocyte-derived exosomes in Alzheimer's disease. *FASEB J.* **30**, 3853–3859. <https://doi.org/10.1096/fj.201600756R> (2016).
41. Wang, J. *et al.* Extracellular vesicles mediate the communication of adipose tissue with brain and promote cognitive impairment associated with insulin resistance. *Cell Metab.* **34**, 1264–1279e8. <https://doi.org/10.1016/j.cmet.2022.08.004> (2022).
42. Rinaudo, M. *et al.* Hippocampal estrogen signaling mediates sex differences in retroactive interference. *Biomedicine* **10**(6), 1387. <https://doi.org/10.3390/biomedicine10061387> (2022).
43. Licursi, V., Conti, F., Fiscon, G. & Paci, P. MIENTURNET: An interactive web tool for microRNA-target enrichment and network-based analysis. *BMC Bioinform.* **20**, 545. <https://doi.org/10.1186/s12859-019-3105-x> (2019).
44. Spinelli, M. *et al.* Neural stem cell-derived exosomes revert HFD-dependent memory impairment via CREB-BDNF signalling. *Int. J. Mol. Sci.* **21**(23), 8994. <https://doi.org/10.3390/ijms21238994> (2020).

Acknowledgements

The authors would like to acknowledge the contribution of Experimental Models Research Core Facility G-STeP of Fondazione Policlinico Universitario “A. Gemelli” IRCCS.

Author contributions

S. F. and C. G. contributed to the study conception and design. M. S., A. R. and A. D. performed material preparation. M. S., F. N., and A. R. performed data collection. F. S. and C. C. carried out bioinformatic analyses. M. S., F. S., C. C., and F. N. performed data analyses. S. F., M. S., F. S. and C. C. wrote the first draft of the manuscript. C. G. and A. F. revised and commented on previous version of the manuscript. All authors read and approved the final manuscript.

Funding

This research was funded by Ministero della Salute-Ricerca Corrente Fondazione Policlinico Universitario A. Gemelli IRCCS (to Claudio Grassi) and Ministero dell'Università e della Ricerca, PRIN 2017 (grant number: 20178YTNWC to Chiara Cencioni and 2017S55RXB to Antonella Farsetti), PRIN 2022 funded from European Union – Next Generation EU (grant number: 20229JKZR4 to Francesco Spallotta).

Competing interests

The authors declare no competing interests.

Additional information

Supplementary Information The online version contains supplementary material available at <https://doi.org/10.1038/s41598-024-69707-7>.

Correspondence and requests for materials should be addressed to S.F.

Reprints and permissions information is available at www.nature.com/reprints.

Publisher's note Springer Nature remains neutral with regard to jurisdictional claims in published maps and institutional affiliations.

Open Access This article is licensed under a Creative Commons Attribution-NonCommercial-NoDerivatives 4.0 International License, which permits any non-commercial use, sharing, distribution and reproduction in any medium or format, as long as you give appropriate credit to the original author(s) and the source, provide a link to the Creative Commons licence, and indicate if you modified the licensed material. You do not have permission under this licence to share adapted material derived from this article or parts of it. The images or other third party material in this article are included in the article's Creative Commons licence, unless indicated otherwise in a credit line to the material. If material is not included in the article's Creative Commons licence and your intended use is not permitted by statutory regulation or exceeds the permitted use, you will need to obtain permission directly from the copyright holder. To view a copy of this licence, visit <http://creativecommons.org/licenses/by-nc-nd/4.0/>.

© The Author(s) 2024